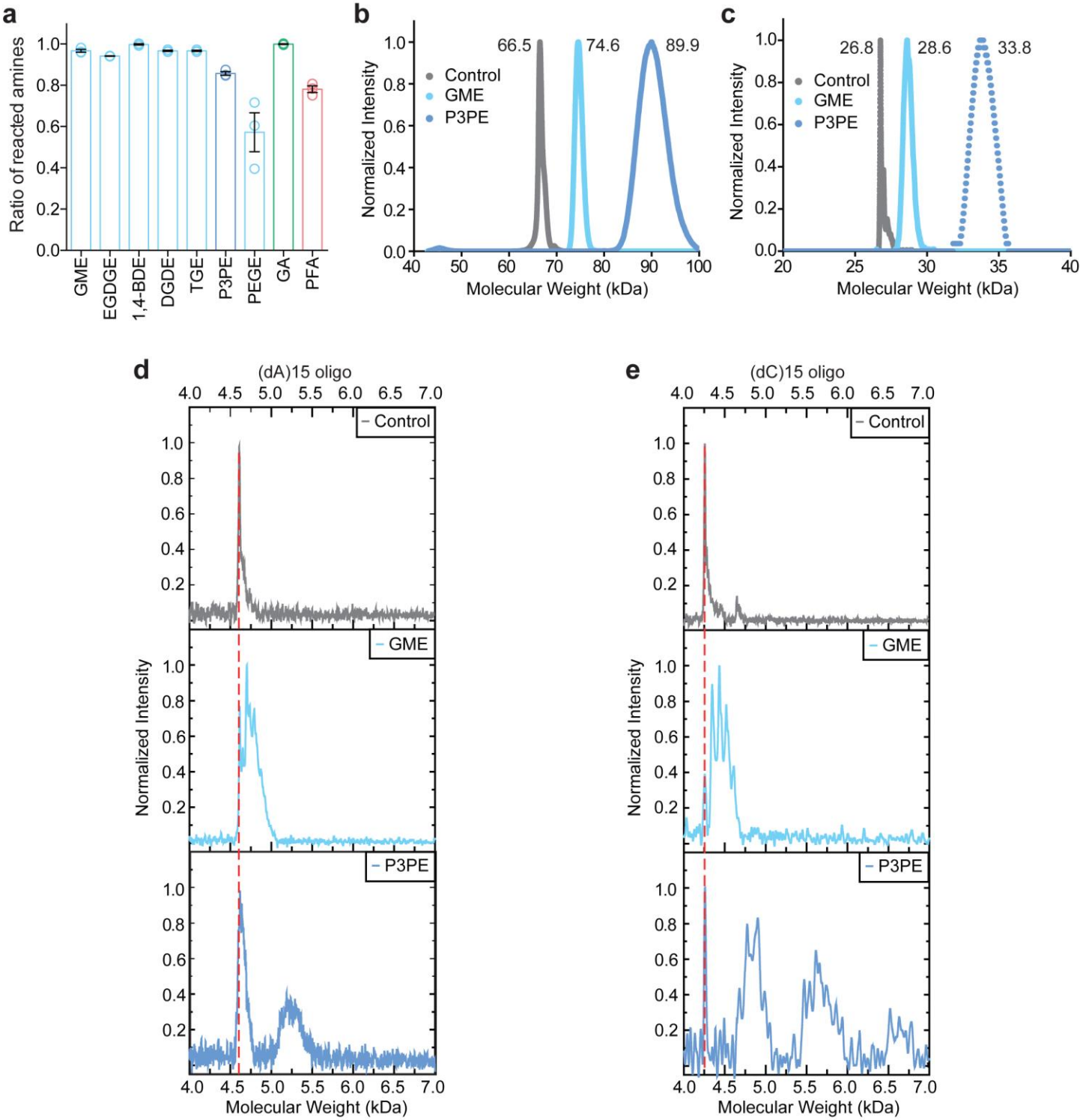

Supplementary Figure 1

Mass spectrometry characterization of epoxide reactions.

(**a**) Degree of amine reactivity of bovine serum albumin (BSA) with epoxide molecules having different numbers of epoxide groups: 1 (GME), 2 (EGDGE, 1,4-BDE, DGDE), 3 (TGE), 4 (PEGE), 5 (P3PE) and with paraformaldehyde (PFA) and glutaraldehyde (GA). N=3

independent experiments. Mean +/- standard error mean was used for this bar graph. (**b**-**c**) MALDI-TOF spectra of BSA (**b**) or GFP (**c**) reacted with GME and P3PE. Corresponding mass shifts indicate a total of ~92 GME or ~45 P3PE molecules crosslinked with BSA, implying that single covalently attached P3PE molecules bridges ~2 epoxide-reactive residues (**b**). A similar calculation shows that roughly 1.5 available epoxide-reactive GFP side-chains are bridged by P3PE (**c**). Mass peak values are indicated as numbers in kDa. (**d, e**) DNA oligos reacted with epoxides at the reaction conditions used for tissue processing (pH 10, 0.1 M sodium carbonate buffer). MALDI-TOF spectra of $(dA)_{15}$ (**d**) and $(dC)_{15}$ oligos (**e**) show mass shifts associated respectively with multiple GME or P3PE epoxide crosslinks, respectively. Peak broadening was observed for P3PE crosslinked oligos indicating the formation of abundant salt adducts with polydisperse P3PE.

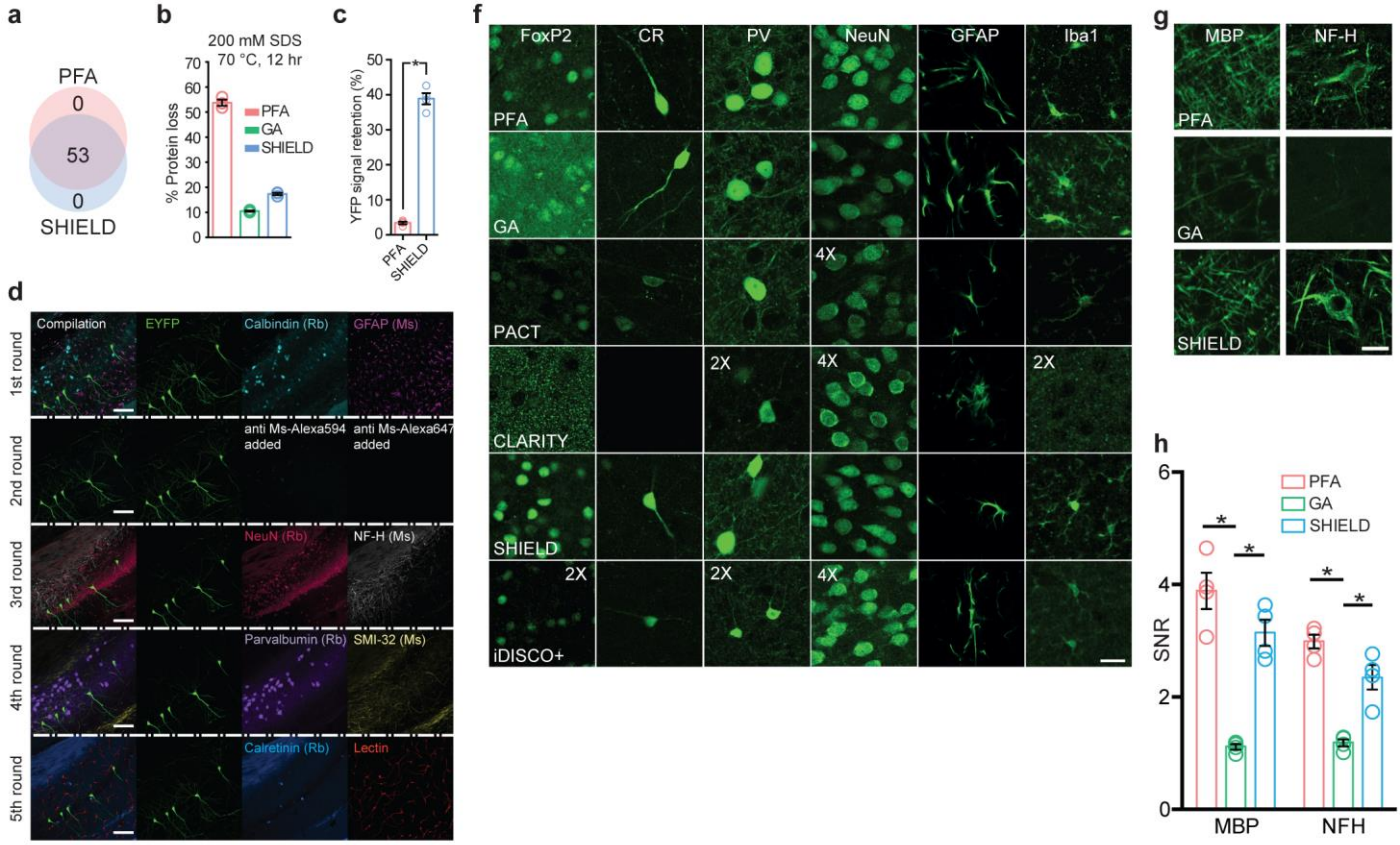
a
PFA
0
53
0
SHIELD
b
200 mM SDS
70 °C, 12 hr
% Protein loss
PFA
GA
SHIELD
c
YFP signal retention (%)
PFA
SHIELD
d
1st round
Compilation
EYFP
Calbindin (Rb)
GFAP (Ms)
2nd round
anti Ms-Alexa594 added
anti Ms-Alexa647 added
3rd round
NeuN (Rb)
NF-H (Ms)
4th round
Parvalbumin (Rb)
SMI-32 (Ms)
5th round
Calretinin (Rb)
Lectin
f
FoxP2
CR
PV
NeuN
GFAP
Iba1
PFA
GA
PACT
CLARITY
SHIELD
iDISCO+
2X
4X
g
MBP
NF-H
PFA
GA
SHIELD
h
SNR
PFA
GA
SHIELD
MBP
NFH

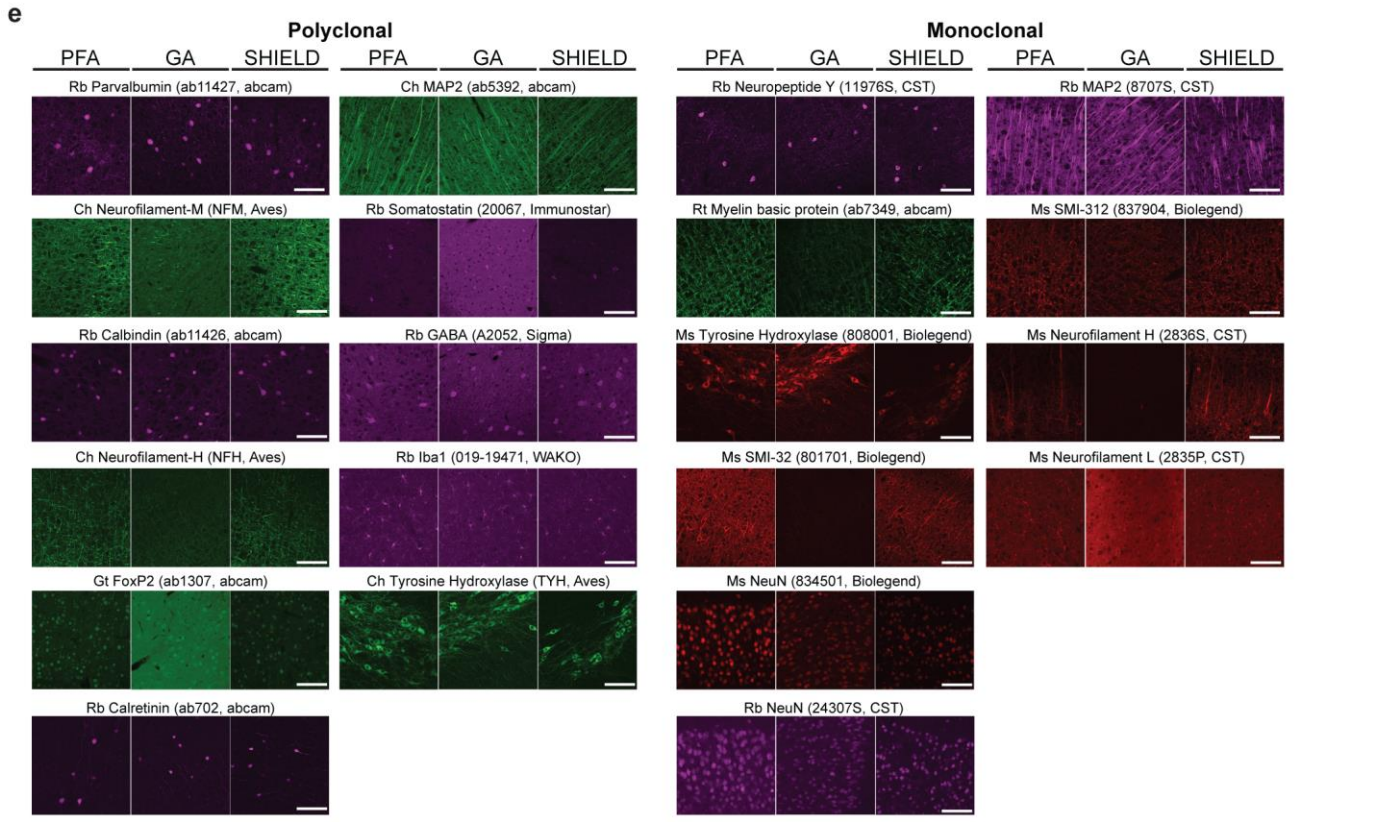
e
Polyclonal
Monoclonal
PFA
GA
SHIELD
Rb Parvalbumin (ab11427, abcam)
Ch MAP2 (ab5392, abcam)
Ch Neurofilament-M (NFM, Aves)
Rb Somatostatin (20067, Immunostar)
Rb Calbindin (ab11426, abcam)
Rb GABA (A2052, Sigma)
Ch Neurofilament-H (NFH, Aves)
Rb Iba1 (019-19471, WAKO)
Gt FoxP2 (ab1307, abcam)
Ch Tyrosine Hydroxylase (TYH, Aves)
Rb Calretinin (ab702, abcam)
Rb Neuropeptide Y (11976S, CST)
Rb MAP2 (8707S, CST)
Rt Myelin basic protein (ab7349, abcam)
Ms SMI-312 (837904, Biolegend)
Ms Tyrosine Hydroxylase (808001, Biolegend)
Ms Neurofilament H (2836S, CST)
Ms SMI-32 (801701, Biolegend)
Ms Neurofilament L (2835P, CST)
Ms NeuN (834501, Biolegend)
Rb NeuN (24307S, CST)

Supplementary Figure 2

Preservation of endogenous proteins and their probe-binding affinities in SHIELD tissue.

(**a**) Venn diagram of antigenicity test results. All 53 tested antibodies compatible with PFA-fixed control tissue worked in SHIELD tissue. (**b**) Protein loss assay in the high-temperature tissue clearing condition (200 mM SDS, 70°C, 12 hr). N = 3 tissues. (**c, d**) FP preservation in SHIELD-processed tissues after multiple rounds of staining and destaining. (**c**) Endogenous YFP signal retention of PFA and SHIELD tissues after destaining treatments corresponding to 5 rounds of stainings. N=4 tissues. (**d**) Multiround staining images from the hippocampal region. Break lines indicate destaining steps. For the second round, secondary antibodies were added to confirm complete unbinding of the primary antibodies imaged at the first round. Thy1-H+ YFP mouse SHIELD tissue was used. Scale bars = 100 μm (**e**) Representative 21 immunofluorescence images in PFA, GA, and SHIELD-processed tissues. Scale bar = 100 μm. The same imaging and display settings were used for each antibody. (**f**) The contrast-adjusted reproduction of Figure 2**i**. The selected images were adjusted for better visual comparison. Scale bar = 20 μm (**g**) Representative images comparing the immunofluorescence of MBP and NF-H in uncleared PFA, GA, and SHIELD tissues. To exclude the effect of tissue clearing on antigenicity, uncleared sections were used. Scale bar = 20 μm. MBP, myelin basic protein; NF-H, neurofilament-H. (**h**) SHIELD maintained a SNR of MBP and NF-H immunofluorescences similar to that of the PFA-control in immunohistochemistry, indicating minimal epitope damage by P3PE crosslinking. N = 4 tissues. Unpaired T-test, $*P < 0.05$. Mean +/- standard error mean was used for all the bar graphs.

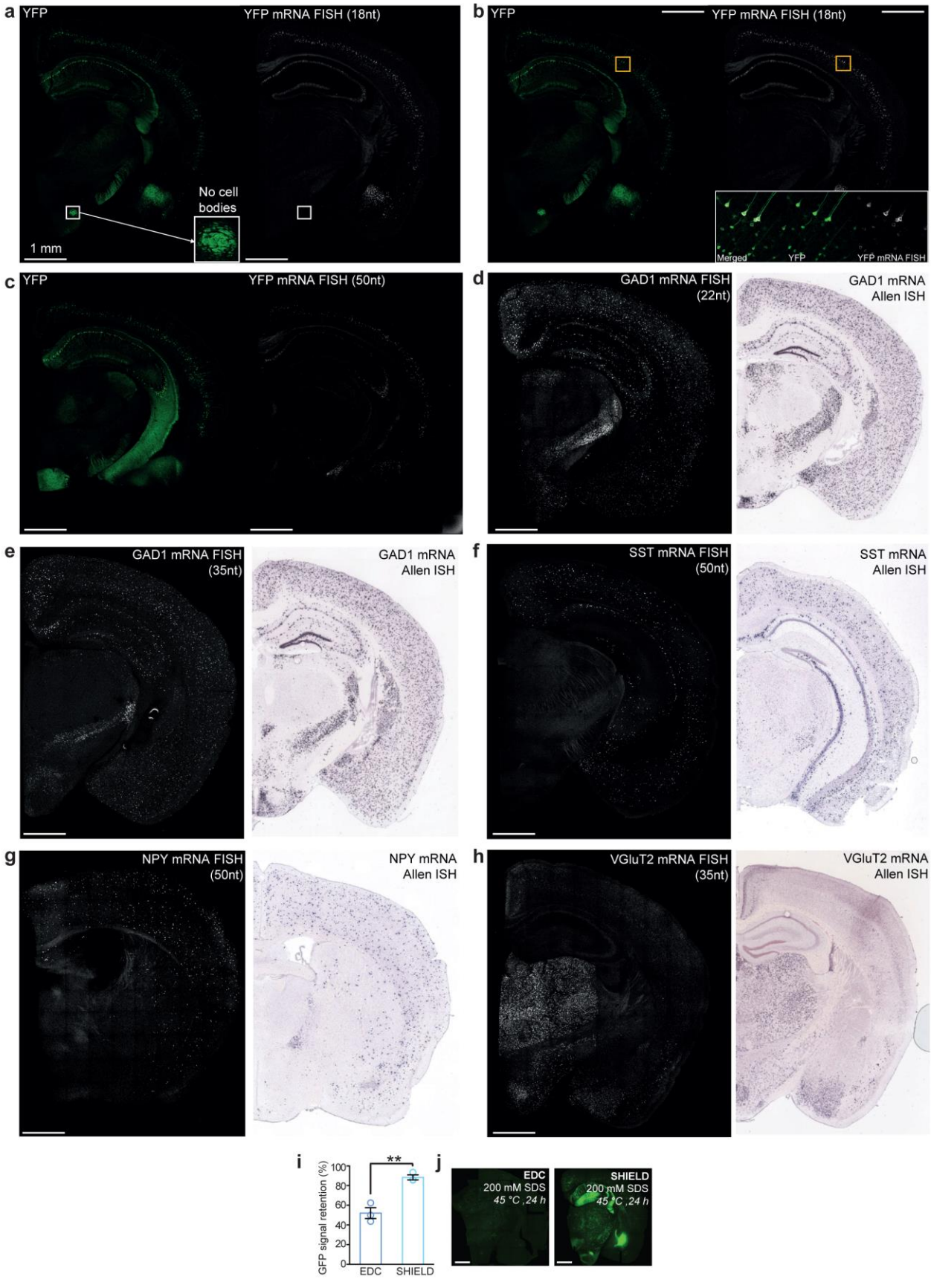
a
YFP
YFP mRNA FISH (18nt)
No cell bodies
1 mm
b
YFP
YFP mRNA FISH (18nt)
Merged
YFP
YFP mRNA FISH
c
YFP
YFP mRNA FISH (50nt)
d
GAD1 mRNA FISH (22nt)
GAD1 mRNA Allen ISH
e
GAD1 mRNA FISH (35nt)
GAD1 mRNA Allen ISH
f
SST mRNA FISH (50nt)
SST mRNA Allen ISH
g
NPY mRNA FISH (50nt)
NPY mRNA Allen ISH
h
VGluT2 mRNA FISH (35nt)
VGluT2 mRNA Allen ISH
i
GFP signal retention (%)
100
80
60
40
20
0
**
EDC
SHIELD
j
EDC
200 mM SDS
45 °C ,24 h
SHIELD
200 mM SDS
45 °C ,24 h

Supplementary Figure 3

Detection of transcripts in SHIELD tissue by fluorescence *in situ* hybridization–hybridization chain reaction (FISH-HCR) with various probe designs.

(**a-c**) FISH-HCR with 18 nt (**a-b**) and 50 nt (**c**) probes for YFP mRNA. The endogenous YFP fluorescence signal was well co-localized with FISH Cy5 signals in individual cells. (**d-h**) FISH-HCR on mRNA transcripts of cell-type marker proteins and their corresponding ISH images from the Allen brain atlas (© 2015 Allen Institute for Brain Science. Allen Brain Atlas API. Available from: brain-map.org/api/index.html). (**d, e**) FISH-HCR for glutamate decarboxylase (GAD1, an inhibitory neuronal marker) using 22nt (**d**) and 35nt (**e**) probes. (**f**) Somatostatin (SST), (**g**) neuropeptide Y (NPY), and (**h**) vesicular glutamate transporter (vGluT2, an excitatory neuronal marker) mRNAs were successfully detected by FISH-HCR in cleared SHIELD-tissue. Scale bar = 1 mm. (**i, j**) GFP signal was preserved better in SHIELD tissue than in tissues processed with EDC (1-ethyl-3-(3-dimethylaminopropyl) carbodiimide hydrochloride) after clearing. (**i**) Bar graph. Unpaired T-test, $^{**}P<0.01$. N=3 tissues. (**j**) Representative images. Scale bar = 1 mm. Mean +/- standard error mean is used for this graph. Data in panel **j** was repeated 3 times independently to make a bar graph in panel **i**.

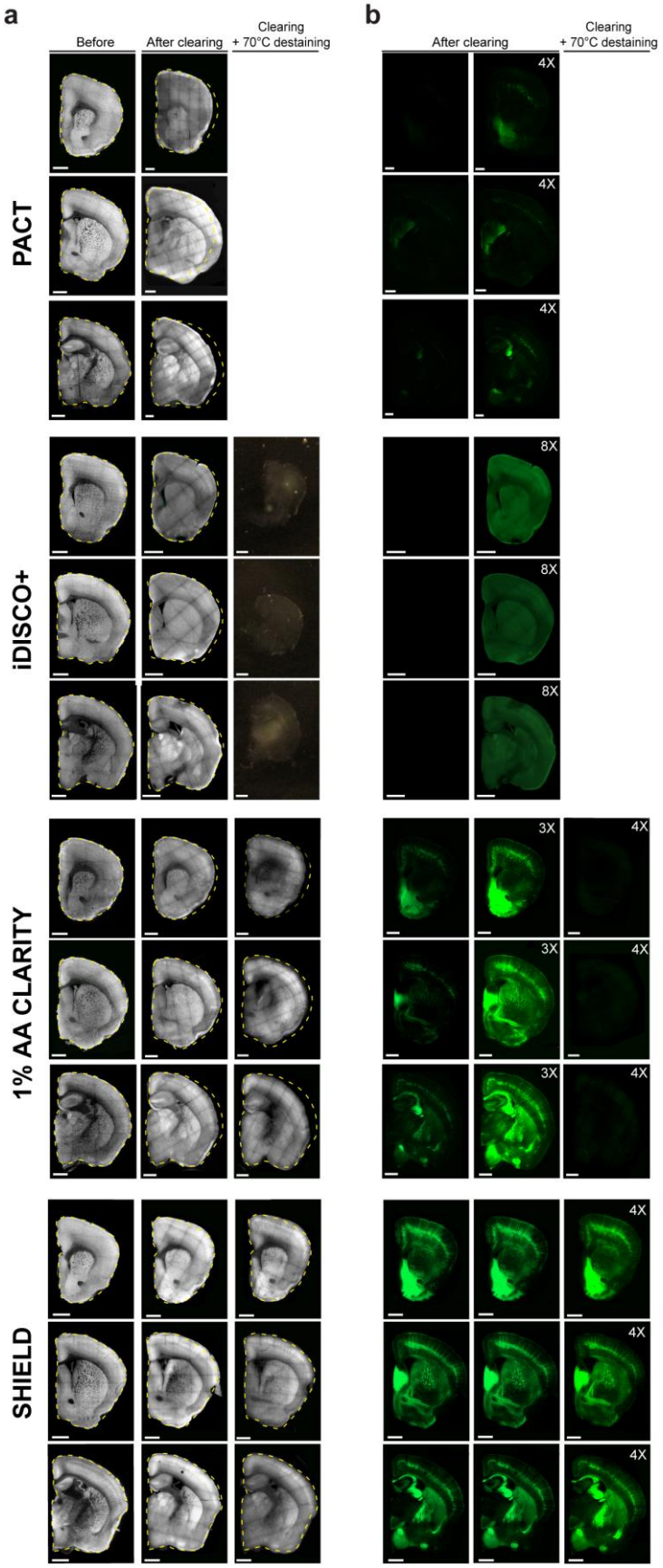
a
b
Before
After clearing
Clearing
+ 70°C destaining
After clearing
Clearing
+ 70°C destaining
PACT
iDISCO+
1% AA CLARITY
SHIELD
4X
8X
3X
4X

Supplementary Figure 4

Structural integrity of SHIELD tissue.

(**a-b**) Autofluorescence (**a**) and YFP (**b**) images of 1mm-thick tissues from different anatomical coordinates of mouse brain hemisphere before and after clearing, and after additional 70°C destaining step (300mM SDS, 2 hr). Images that were not included in Figure 3a are presented here. The contour of the uncleared sections are marked with yellow dotted lines in subsequent images. In YFP images, numbers on the top right corners indicate the intensity gain from image display range. PACT images after 70°C destaining step are not included because the tissues melted. Scale bars = 1 mm.

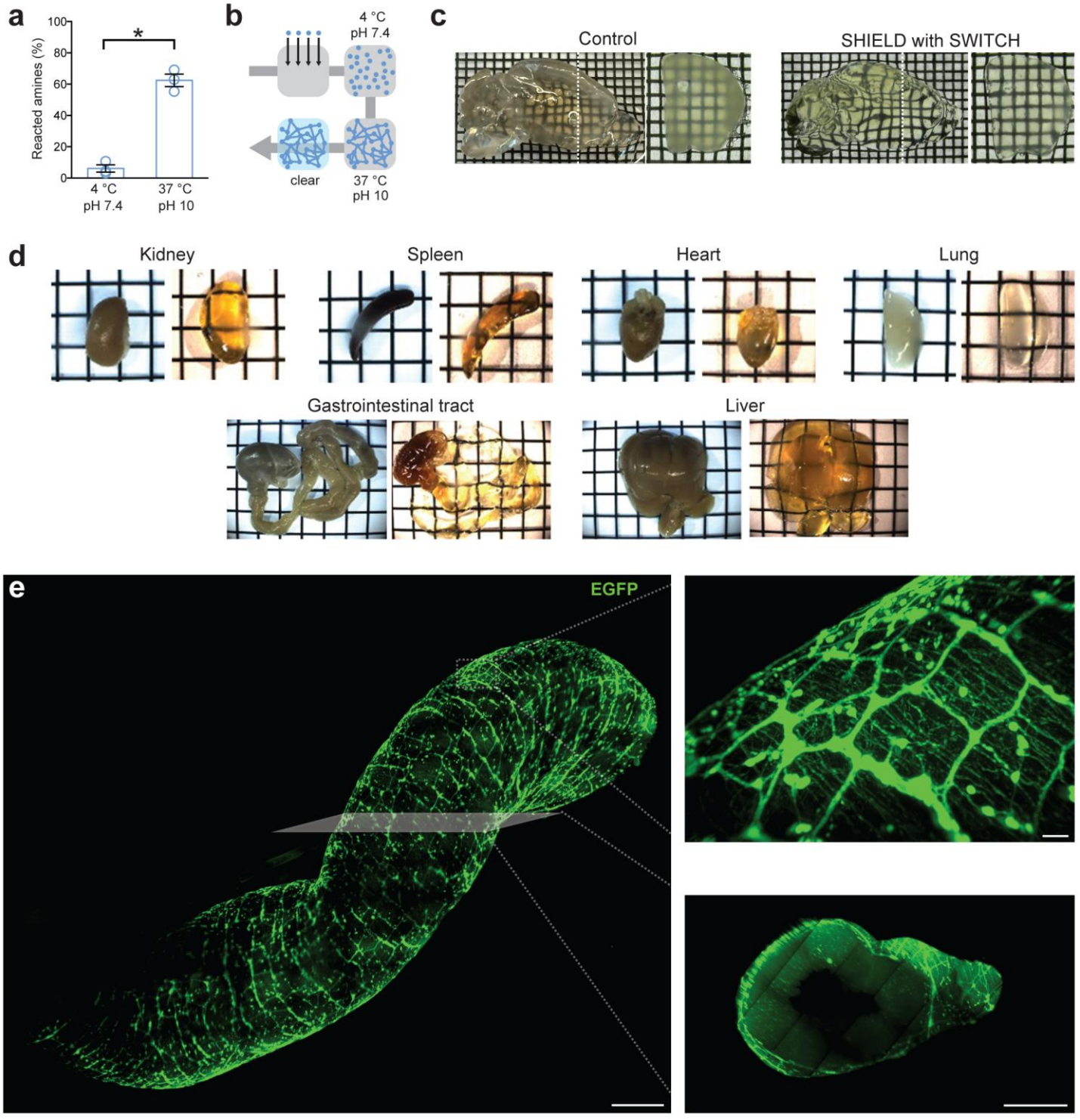

Supplementary Figure 5

Whole organ processing and clearing with SHIELD.

(**a**) SWITCH chemistry in SHIELD processing. Epoxy-amine reactivity at 37°C pH 10 condition (SWITCH-ON) was 10-fold higher than reactivity at 4°C pH 7.4 condition (SWITCH-OFF). Unpaired T-test, *P < 0.05, N = 3 independent experiments. Mean +/- standard error mean is used for this bar graph. (**b**) Schematic diagram of whole organ SHIELD processing using SWITCH chemistry. The initial incubation of tissue in the SWITCH-OFF condition ensures complete and homogeneous distribution of epoxide molecules across the

tissue volume. Subsequent SWITCH-ON condition initiates synchronized crosslinking throughout the tissue volume. (**c**) Comparison of SHIELD tissue processed with (*right*) or without SWITCH (*left*). Note that the control sample shows opaque tissue layer at its surface even after clearing, suggesting overfixation at the tissue surface. SHIELD tissue fixed with SWITCH chemistry is uniformly transparent throughout its volume after clearing. Grid = 1 mm. (**d**) SHIELD-processed mouse organs before (*left panels*) and after clearing (*right panels*). Grid = 1 mm. (**e**) 3D visualization of an intestine of ChAT-EGFP transgenic mouse showing processes of $ChAT^{+}$ motor neurons innervating the intestine. Scale bars = 1 mm (*left, lower right*), 50 μm (*upper right*).